PHILOSOPHICAL MAGAZINE B, 2001, VOL. 81, NO. 4, 365–376

Calculation of plasmonic dispersion in quantum wires: angular degeneracy and shape-confinement effects

F. LIGUORI†, F. BUONOCORE, D. NINNO and G. IADONISI

Istituto Nazionale per la Fisica della Materia and Dipartimento di Scienze Fisiche, Università di Napoli Federico II, Complesso Universitario di Monte S. Angelo, Via Cintia, I-80126 Naples, Italy

[*Received 16 May 2000 and accepted 15 November 2000*]

ABSTRACT

We present a random-phase approximation calculation of the collective plasmon excitation spectrum of a one-dimensional electron gas confined in cylindrical and rectangular semiconductor quantum wires. The plasmon spectrum for the cylindrical case is calculated considering up to three occupied subbands. Taking into account the twofold angular degeneracy of the single-particle energy spectrum, we derive different expressions for the electron–electron interaction when opposite angular quantum numbers are involved. That occurrence leads, even in a two-subband system, to the presence of new undamped plasmon modes for $q \rightarrow 0$ not exhibited in previous work. Comparing plasmon modes between cylindrical and rectangular quantum wires, we find an investigable shape-confinement effect for the intrasubband plasma excitation in the lowest subband.

§1. INTRODUCTION

In recent years, the study of low-dimensional systems (quantum wells, wires or dots) has been the subject of great activity from both theoretical and experimental points of view (Ando *et al.* 1982, Kotthaus 1988, Stern 1993). The main physical properties of these systems have been very extensively studied (Das Sarma and Lai 1985, Lee and Spector 1985, Gold and Ghazaly 1990a,b, Hu and O'Connel 1990, Li and Das Sarma 1991, Wendler *et al.* 1991, Li *et al.* 1992, Proetto 1992, Hwang and Das Sarma 1994, Wendler and Grigoryan 1994, Agosti *et al.* 1998, Das Sarma and Hwang 1999) in the general context of condensed-matter theory and compared with their three-dimensional counterparts. In one-dimensional systems, the energy–momentum conservation law is more restrictive on the single-particle continuum than in two- or three-dimensional structures, so increasing the relative weight of the undamped collective excitations. It is therefore of great importance to study the effect of the confinement on the excitation (plasmon and single-particle) spectrum in a quasi-one-dimensional electron gas (Q1DEG).

The aim of this paper is the study of the plasma excitations at zero temperature of a Q1DEG in a semiconductor quantum wire with different confining shapes, namely cylindrical and rectangular shapes. Specifically, the multisubband occupancy, the role of the angular degeneracy, the inclusion of upper empty subbands

†Email: fliguori@libero.it

Philosophical Magazine B ISSN 1364–2812 print/ISSN 1463–6417 online
http://www.tandf.co.uk/journals
DOI: 10.1080/13642810010022938

in the electron gas and the effects of the shape confinement have attracted our interest.

The model that we adopt makes use of the effective-mass approximation with hard-wall boundary conditions for the single-particle spectrum (Lee and Spector 1985, Gold and Ghazaly 1990a,b, Wendler *et al.* 1991, Hwang and Das Sarma 1994, Wendler and Grigoryan 1994, Mutluay and Tanatar 1997, Agosti *et al.* 1998, Das Sarma and Hwang 1999). A more refined approach which takes into account a soft confining potential has been considered within a Hartree scheme (Yu and Hermanson 1990, Proetto 1992, Wendler and Haupt 1995, Reboredo and Proetto 1997). We have developed a multisubband random-phase approximation (RPA) dielectric matrix according to the self-consistent field (SCF) method (Ehrenreich and Cohen 1959).

For the cylindrical quantum wire (CQW), we have calculated plasmon modes considering up to three occupied subbands, examining also the intermediate case of a CQW with the two lowest subbands being occupied and the third empty. To the best of our knowledge, calculation of the three-occupied-subband case has not been published before for a CQW. However, it must be stressed that calculations considering two occupied subbands in a CQW has been examined (Wendler and Grigoryan 1994), whereas, for different geometrical configurations, such as rectangular, zero-thickness and harmonically confined structures, there is a vast literature with even more than three occupied subbands (Hu and O'Connel 1990, Yu and Hermanson 1990, Haupt *et al.* 1991, Li and Das Sarma 1991, Wendler *et al.* 1991, Reboredo and Proetto 1994, Wendler and Haupt 1995, Borges *et al.* 1997, Mutluay and Tanatar 1997).

Unlike previous work, we take properly into account, when allowed by the symmetry-induced selection rules, the effective interaction between electronic states with opposite angular quantum numbers. The inclusion of these interactions may add new plasmon modes to the spectrum, even within the two-occupied-subband model.

Finally, we compare the above results of the CQW with those of a rectangular quantum wire (RQW). It is well known (Gold and Ghazaly 1990a, Stern 1993) that quantities averaged over the wavefunctions, such as the electron–electron and the electron–impurity interactions, as well as the impurity binding energy and the mobility, depend mainly on the cross-section area and only weakly on the geometrical shape. No suggestion has been made about a possible candidate for an observable property in the plasmon spectrum depending on the confinement geometry. We propose a systematic analysis for both the interaction matrix elements and the plasmon modes where the relevant shape effect on plasma excitation modes is analysed. In this analysis, care has been taken with regard to the respective selection rules for the coupling of intrasubband and intersubband plasmons.

§2. Angular degeneracy in the multisubband dielectric matrix in a cylindrical quantum wire

We consider a degenerate Q1DEG totally confined (zero boundary conditions for the wavefunctions) in a CQW of radius R and length L, oriented along the z axis, and we neglect the effects of the image potential. Linear response theory, in the RPA framework and following the SCF method (Ehrenreich and Cohen 1959), is well established. The multisubband dielectric matrix is

$$\varepsilon_{\beta_1\beta_2\beta\beta'}(q,\omega) = \delta_{\beta\beta_2}\delta_{\beta'\beta_1} - V_{\beta_1\beta_2\beta\beta'}(q)X_{\beta\beta'}(q,\omega), \tag{1}$$

where $X_{\beta\beta'}(q,\omega)$ is the RPA polarization function, $\beta = (\pm l, n)$ are the subband indices (l and n are the angular and the radial quantum numbers respectively) and $V_{\beta_1\beta_2\beta\beta'}(q)$ is the effective electron–electron interaction potential averaged over the planar wavefunctions. The condition

$$\det \|\varepsilon_{\beta_1\beta_2\beta\beta'}(q,\omega)\| = 0 \tag{2}$$

defines the dispersion relations for the plasmons in the wire. With the contribution of only a few subbands, this determinantal problem becomes tractable. Moreover, the use of the selection rule induced by the cylindrical symmetry, namely $V_{l_1n_1,l_2n_2;l_3n_3,l_4n_4}(q) = 0$ of $l_1 - l_2 \neq -(l_3 - l_4)$ for the interaction elements, makes possible the decoupling of equation (2) into the subdeterminants $D_{\Delta l}(q,\omega) = 0$, each defined by a value of $\Delta l = l_1 - l_2 = l_4 - l_3$. It is easy to prove that subdeterminants with $+\Delta l$ and $-\Delta l$ lead to the same dispersion relations. From the above selection rules, equation (2) takes the diagonal block form

$$\begin{aligned}\det\|\varepsilon_{\beta_1\beta_2\beta\beta'}\| &= \prod_{\Delta l=-\infty}^{\infty} D_{\Delta l}(q,\omega) \\ &= D_0(q,\omega) \prod_{|\Delta l|=1}^{\infty} [D_{|\Delta l|}(q,\omega)]^2 \\ &= 0.\end{aligned} \tag{3}$$

Thus we solve a finite set of decoupled equations, such as $D_{|\Delta l|}(q,\omega) = 0$, each describing the dispersion of the 'angular plasmon' $|\Delta l|$. Analytical expressions for the interaction elements are not yet available, although the polynomial approximation (Gold and Ghazali 1990a,b) for the radial part of the wavefunctions gives excellent agreement with full numerical calculations. The intrasubband (i.e. with $\Delta l = 0$) and intersubband (i.e. with $\Delta l \neq 0$) plasmons strongly depend on the long-wavelength behaviour of the interaction elements. It is well known that to leading order in qR we have $V(qR) \simeq -(2e^2/\varepsilon_L)b\ln(qR)$ if $|\Delta l| = 0$ and $V(qR) \simeq (2e^2/\varepsilon_L)a \neq 0$ if $|\Delta l| \neq 0$ where ε_L is the dielectric constant of the background, and a and b are constants. Matrix elements connecting states with opposite values of the angular quantum number l provide a peculiar situation, because new plasmon modes are related to them. For instance, let us consider a wire with two subbands, both occupied. In this system, there are two plasmon modes with a q-linear dependence. The first, with $|\Delta l| = 0$, is well known (Wendler and Grigoryan 1994) and has the dispersion relation

$$\omega_0(q) \approx \frac{\hbar}{m}\left(k_{F0}k_{F1}\frac{2k_{F0} + k_{F1}}{k_{F0} + 2k_{F1}}\right)^{1/2} q, \tag{4}$$

with $k_{F|l|}$ the Fermi wave-vector and m the band mass. The second, with $|\Delta l| = 2$, originates from the $l = \pm 1$ degeneracy through the dispersion equation $1 - V_{1\bar{1}\bar{1}1}X_{1\bar{1}} = 0$, whose $q \to 0$ solution is

$$\omega_{1\bar{1}}(q) \approx \left(\frac{\hbar^2 k_{F1}^2}{m^2} + \frac{2k_{F1}}{\pi m} V_{1\bar{1}\bar{1}1}(q \approx 0)\right)^{1/2} q, \tag{5}$$

where $V_{1\bar{1}\bar{1}1}(q \approx 0) \approx (2e^2/\varepsilon_L)[0.1362 + O(q^2)]$.

§3. A cylindrical quantum wire with three subbands: the 012^0 model

Hereafter, a sequence of integers, such as $01, \ldots, s, \ldots, s_{max}$, denotes the set of subbands involved in the model of wire under study, each integer s referring to the $|l|$ value of the subband and the symbol s^0 meaning that the sth subband is empty. In the three-subband model, two cases are possible (at $T = 0\,$K) beyond the two-occupied-subband (01 model). If $E_{1,1} < E_F < E_{2,1}$, it is the 012^0-model and, if $E_{1,1} < E_{2,1} < E_F < E_{0,2}$, it is the 012 model. E_F and $E_{|l|,n}$ are the Fermi level and the bottom energy of the subband $(|l|, n)$ respectively.

This 012^0 case is useful to explain the effect of the upper empty subband on the plasmon branches in the strictly 01 model. We choose $E_F = \frac{15}{9}\,\mathrm{Ryd}^*$ and $R = 3a^*$, where $1\,\mathrm{Ryd}^* = \hbar^2/2ma^{*2}$ and $a^* = \varepsilon_L \hbar^2/me^2$ are the effective Rydberg and Bohr radius respectively. The bottom of the second subband is at an energy $E_{1,1} \approx 14.682/9\,\mathrm{Ryd}^*$. For a GaAs wire, we have $1\,\mathrm{Ryd}^* \approx 5.44\,\mathrm{meV}$ and $a^* \approx 10.282\,\mathrm{nm}$, and therefore $R \approx 30.846\,\mathrm{nm}$ with a linear electron density $n \approx 8.594 \times 10^5\,\mathrm{cm}^{-1}$. The dispersion relations (3) are

$$D_0(q,\omega) = (1 - V_{0000}X_{00})(1 - V_{1111}2X_{11}) - V^2_{\bar{1}100}X_{00}2X_{11} = 0, \tag{6}$$

$$D_1(q,\omega) = (1 - V_{0110}\Pi_{10})(1 - V_{1221}\Pi^0_{21}) - V^2_{0121}\Pi_{10}\Pi^0_{21} = 0, \tag{7}$$

$$D_2(q,\omega) = (1 - V_{1\bar{1}\bar{1}1}X_{11})(1 - V_{0220}\Pi^0_{20}) - V^2_{1\bar{1}02}X_{11}\Pi^0_{20} = 0, \tag{8}$$

$$D_3(q,\omega) = 1 - V_{\bar{1}22\bar{1}}\Pi^0_{21} = 0. \tag{9}$$

Thus plasma excitations with $|\Delta l| = 0, 1, 2, 3$ are possible. In the above equations, the radial index $n \equiv 1$ is dropped. X_{00} ($2X_{|l|\,|l|}$ if $l \neq 0$) is the intrasubband RPA polarization function for the $l = 0$ ($l \neq 0$) subband and $\Pi_{|l_1|\,|l_2|}$ is the intersubband polarization function for the (l_1, l_2) subband pair. The superscript 0 in Π^0 indicates the presence of the empty subband $|l| = 2$.

The two coupled intrasubband modes with $|\Delta l| = 0$ (equation (6)) are not modified by the higher empty subband and their dispersion laws are well known (Wendler and Grigoryan 1994). For instance, the lower branch has a frequency given by equation (4) at $q \to 0$.

If $|\Delta l| = 1$ (equation (7)) there are three intersubband modes related to the matrix elements $l = 0 \leftrightarrow l = \pm 1$ coupled to the $l = \pm 1 \leftrightarrow l = \pm 2$ matrix elements. Only the highest-energy mode is very sensitive to the presence of the empty subband. To see this, we consider the two higher plasmon branches, which at $q \approx 0$ arise from the coupling of the two modes

$$\begin{aligned} \hbar\omega_{10}(0) &\equiv (\Delta E^2_{10} + \hbar^2\Omega^2_{\mathrm{dp},10})^{1/2}, \\ \hbar\omega_{21}(0) &\equiv (\Delta E^2_{21} + \hbar^2\Omega^2_{\mathrm{dp},21})^{1/2}, \end{aligned} \tag{10}$$

where $\Delta E_{|l_1|\,|l_2|} = E_{|l_1|,1} - E_{|l_2|,1}$ and

$$\hbar^2\Omega^2_{\mathrm{dp},10} = \frac{4(k_{F0} - k_{F1})}{\pi}\, V_{0110}(q \approx 0)\Delta E_{10},$$

$$\hbar^2\Omega^2_{\mathrm{dp},21} = \frac{4k_{F1}}{\pi}\, V_{1221}(q \approx 0)\Delta E_{21},$$

are the depolarization shifts. In equation (10), $\hbar\omega_{10}$ comes from the 01 model (Wendler and Grigoryan 1994) and $\hbar\omega_{21}$ testifies to the presence of the third empty subband. The approximate coupled solutions at $q \approx 0$ are

$$\tilde{\omega}_{\pm}^{[1]}(0) \approx \{\tfrac{1}{2}[\omega_{10}^2(0) + \omega_{21}^2(0)] \pm \tfrac{1}{2}|\omega_{10}^2(0) - \omega_{21}^2(0)|(1 + 4\rho^2\alpha^2)^{1/2}\}^{1/2}, \tag{11}$$

with $\rho^2 = V_{0121}^2(0)/V_{0110}(0)V_{1221}(0) \approx 1$ and $\alpha = \Omega_{\mathrm{dp},10}\Omega_{\mathrm{dp},21}/|\omega_{10}^2(0) - \omega_{21}^2(0)|$. The empty subband acts to push up the frequency $\hbar\omega_{10}$ from 1.476 Ryd* (01 model) to $\hbar\tilde{\omega}_{+}^{[1]}(0) \approx 1.692$ Ryd* (equation (11)). The depolarization shift at $E_{\mathrm{F}} = \frac{15}{9}$ Ryd* is enhanced by a factor of about 1.253. The mode $\hbar\tilde{\omega}_{-}^{[1]}(0)$ is a new plasmon absent in the 01 model. The third solution of equation (7) shows a negative dispersion law of the type $\hbar\tilde{\omega}^{[1]}(q \approx 0) = \Delta E_{10} - \hbar\tilde{\xi}q^2$. The effect of the empty subband on that mode is negligible.

Two free-damping modes have $|\Delta l| = 2$ (equation (8)). Their behaviour at $q \approx 0$ is established through the coupling between the frequencies $\omega_{1\bar{1}}$ (equation (5)), coming from the angular degeneracy, and ω_{20}:

$$\hbar\omega_{20} \equiv (\Delta E_{20}^2 + \hbar^2\Omega_{\mathrm{dp},20}^2)^{1/2},$$
$$\hbar^2\Omega_{\mathrm{dp},20}^2 = \frac{4k_{\mathrm{F}0}}{\pi}\, V_{0220}(q \approx 0)\,\Delta E_{20},$$

so that these modes with $|\Delta l| = 2$ are

$$\tilde{\omega}_{\pm}^{[2]}(q \approx 0) \approx \{\tfrac{1}{2}[\omega_{20}^2(0) + \omega_{1\bar{1}}^2(0)] \pm \tfrac{1}{2}[\omega_{20}^2(0) - \omega_{1\bar{1}}^2(0)](1 + 4u)^{1/2}\}^{1/2},$$
$$u = \frac{\Omega_{\mathrm{dp},20}^2(\omega_{1\bar{1}}^2 - \hbar^2 k_{\mathrm{F}1}^2 q^2/m^2)}{[\omega_{20}^2(0) - \omega_{1\bar{1}}^2(0)]^2}. \tag{12}$$

In this case the coupling is very small, because $u \approx 10^{-4}$–10^{-3} and $\omega_{20} \gg \omega_{1\bar{1}}$ (indeed, for $q \to 0$, $\omega_{20} \neq 0$ while $\omega_{1\bar{1}} \to 0$ as const. q). For the mixed modes $\tilde{\omega}_{\pm}^{[1]}$ (equation (11)), on the contrary, one has $\omega_{10} \simeq \omega_{21}$ and, thus, more efficient coupling. Therefore the modes $\tilde{\omega}_{+}^{[2]}$ and $\tilde{\omega}_{-}^{[2]}$ are very close to the values $\omega_{20}(0)$ and $\omega_{1\bar{1}}(0)$ respectively.

Equation (9) with $|\Delta l| = 3$ admits just one free-damping intersubband mode (collective excitation between states $l = -1$ and $l = 2$). That equation is exactly solvable. At $q \approx 0$ we obtain $\hbar\tilde{\omega}^{[3]} \approx (\Delta E_{21}^2 + \hbar^2\Omega_{\mathrm{dp},21}^2)^{1/2}$, with $\hbar\Omega_{\mathrm{dp},21}^2 = (4k_{\mathrm{F}1}/\pi)V_{\bar{1}22\bar{1}}(0)\,\Delta E_{21}$. This mode is obviously absent in the 01 model.

§4. Cylindrical quantum wire with three subbands: the 012 model

In this case we set $E_{\mathrm{F}} = \frac{27}{9}$ Ryd* and $R = 3a^*$. The electron density in GaAs is $n \approx 2.726 \times 10^6\ \mathrm{cm}^{-1}$. Plasmon modes with $|\Delta l| = 0, 1, 2, 3, 4$ are allowed and the dispersion relations (3) are

$$
\begin{aligned}
D_0(q,\omega) = {} & (1 - V_{0000}X_{00})(1 - V_{1111}2X_{11})(1 - V_{2222}2X_{22}) \\
& - (1 - V_{0000}X_{00})V^2_{1122}2X_{11}2X_{22} - (1 - V_{1111}2X_{11})V^2_{0022}X_{00}2X_{22} \\
& - (1 - V_{2222}2X_{22})V^2_{0011}X_{00}2X_{11} - 2V_{0011}V_{0022}V_{1122}X_{00}2X_{11}2X_{22} \\
= {} & 0,
\end{aligned} \tag{13}
$$

$$D_1(q,\omega) = (1 - V_{0110}\Pi_{10})(1 - V_{1221}\Pi_{21}) - V^2_{0121}\Pi_{10}\Pi_{21} = 0, \tag{14}$$

$$D_2(q,\omega) = (1 - V_{1\bar{1}\bar{1}1}X_{11})(1 - V_{0220}\Pi_{20}) - V^2_{\bar{1}102}X_{11}\Pi_{20} = 0, \tag{15}$$

$$D_3(q,\omega) = 1 - V_{\bar{1}22\bar{1}}\Pi_{21} = 0, \tag{16}$$

$$D_4(q,\omega) = 1 - V_{2\bar{2}\bar{2}2}X_{22} = 0. \tag{17}$$

The three intrasubband modes $\Delta l = 0$ (equation (13)), obtained with the numerical solution of $D_0(q,\omega) = 0$, are plotted in figure 1 as broken curves together with the Landau regions. It is easy to see from the figure that, while the upper curve is everywhere outside the damping region, the two lowest branches are free damping only for small q. For $qR \to 0$, the two lower branches show a linear q dependence (as the lower curve with $\Delta l = 0$ in the 01 model), while the upper branch behaves as $qR[-\ln(qR)]^{1/2}$. It is worth stressing that this is a general result which holds for any number of occupied subbands. For the upper, middle and lower branches, we obtain for $qR \ll 1$

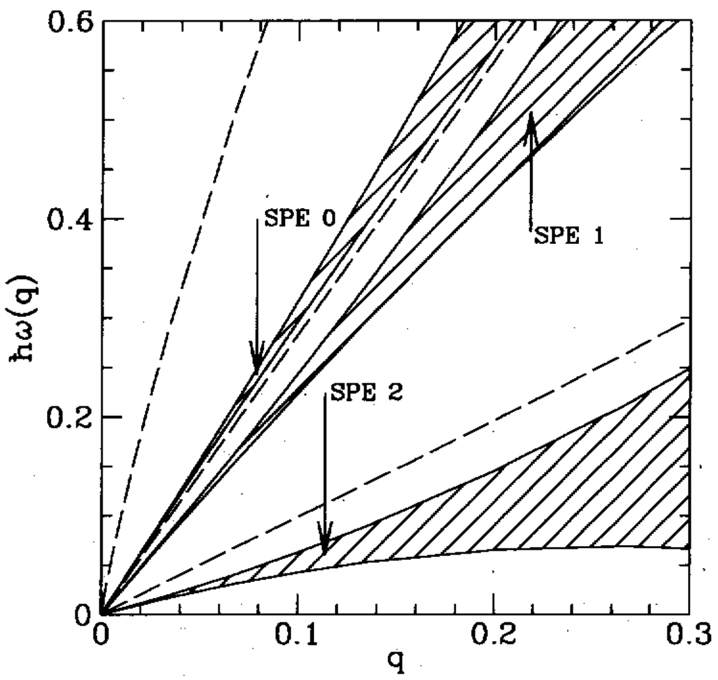

Figure 1. Plasmon dispersion in the CQW of the intrasubband modes with $\Delta l = 0$ in the 012 model. The shaded regions are the single-particle excitation (SPE) continua. The units are $1/a^*$ for q and Ryd* for $\hbar\omega$. The electron linear density $n \approx 2.726 \times 10^6\ \mathrm{cm}^{-1}$ for GaAs.

$$\omega_1^{[0]}(q) \approx \omega_S[-\ln(qR)]^{1/2} qR, \tag{18a}$$

$$\omega_2^{[0]}(q) \approx \frac{\hbar k_{F0}}{m}\left[-\frac{1}{2}+\frac{1}{2}\left(1+8\,\frac{k_{F1}+k_{F2}}{k_{F0}}\right)^{1/2}\right]^{1/2} q, \tag{18b}$$

$$\omega_3^{[0]}(q) \approx \left(\frac{2\hbar^2 k_{F0}k_{F1}k_{F2}}{m^2(k_{F1}+2k_{F0})}\right)^{1/2} q \tag{18c}$$

respectively. In equations (18),

$$\omega_S^2 = 2ne^2/m\varepsilon_L R^2$$

where

$$n = (2/\pi)(k_{F0}+2k_{F1}+2k_{F2})$$

is the linear density. It can be proved that the dependence of $\omega_1^{[0]}$ on q, n and R is a common feature in quantum wires, whatever the number of occupied subbands and the geometry of the confinement. The middle plasmon frequency $\omega_2^{[0]}$ matches the curve obtained from equation (4) when only two subbands are occupied. Finally, the lower frequency $\omega_3^{[0]}$ exists only if $k_{F2} \neq 0$, when even the third subband is populated.

In figure 2 we show the numerically calculated four modes with $|\Delta l| = 1$ (equation (14)), coming from the mixed excitations $l = 0 \leftrightarrow l = \pm 1$ and $l = \pm 1 \leftrightarrow l = \pm 2$. We consider first the two plasma oscillations with positive dispersion (dotted curves). For these modes, equation (11) still holds, but the depolarization shift $\hbar^2\Omega^2_{dp,21}$ is now proportional to $k_{F1} - k_{F2}$, reflecting the occupancy of the third subband. The +

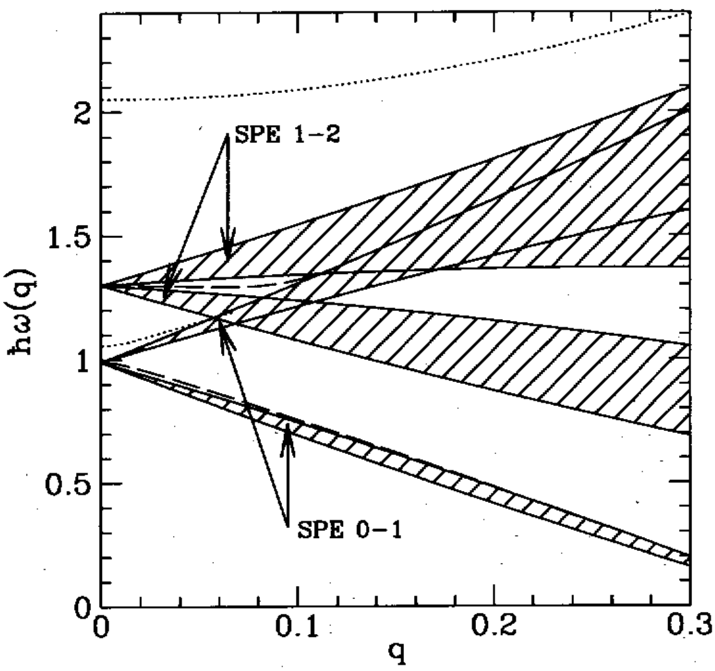

Figure 2. The four intersubband $|\Delta l| = 1$ plasmon branches in the CQW 012 model. The SPE regions, units and density are as in figure 1.

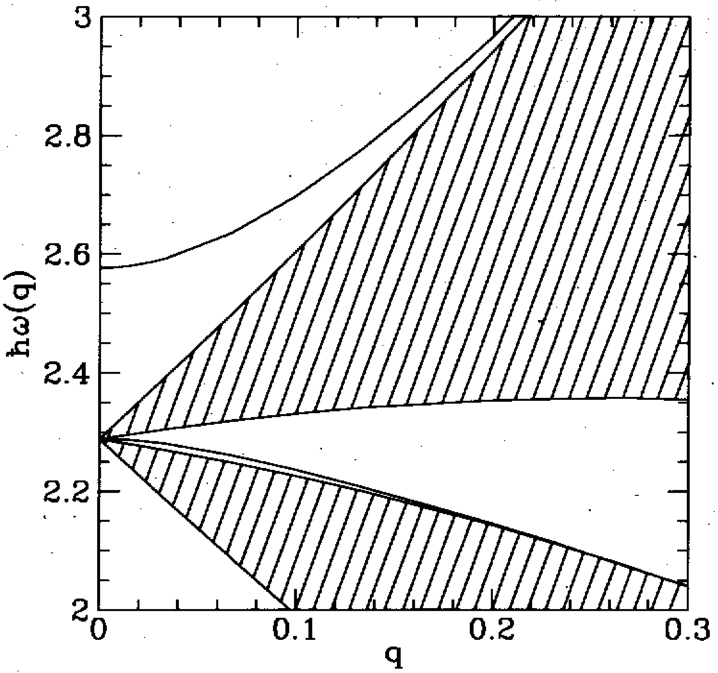

Figure 3. Intersubband $|\Delta l| = 2$ plasmon branches in the CQW 012 model. The SPE regions, units and density are as in figure 1.

sign in equation (11) refers here to the upper curve, and the $-$ sign to the lower curve. The two curves with negative dispersion (broken curves in figure 2) behave for $q \approx 0$ as $\hbar\omega(q) \approx \Delta E - \hbar\bar{\xi}q^2$, where ΔE is the respective subband energy separation.

Three plasmon curves correspond to $|\Delta l| = 2$ (equation (15)), two with positive and one with negative dispersion. For $q \to 0$, the frequencies with positive dispersion are well approximated by equation (12), with the depolarization shift $\hbar\Omega^2_{\mathrm{dp},20}$ now proportional to $k_{\mathrm{F0}} - k_{\mathrm{F2}}$. In figure 3 we plot only the two higher-energy plasmons. Also in this case the coupling effect between the modes ω_{20} and $\omega_{1\bar{1}}$ is very small for all three branches.

For brevity here, no figures for the angular plasmons with $|\Delta l| = 3$ (equation (16)) and with $|\Delta l| = 4$ (equation (17)) are reported. Analytical expressions for these modes can be easily calculated for all q values. If $|\Delta l| = 3$ there are two intersubband branches. If $|\Delta l| = 4$, only one mode exists, very close to the boundary of the Landau zone, with a linear dispersion law at $q \to 0$ as in equation (5) after the replacements $k_{\mathrm{F1}} \to k_{\mathrm{F2}}$ and $V_{1\bar{1}\bar{1}1} \to V_{2\bar{2}\bar{2}2}$. The role played by the angular degeneracy in increasing the number of plasmon modes is quite clear from the above analysis.

§ 5. Rectangular quantum wires

When comparing the electronic states of a RQW (i.e. with a rectangular confining potential shape) and of a CQW with the same cross-section area, it is well known (Stern 1993) that the asymptotic density of states at large quantum numbers depends mainly on the area and only weakly on the geometry, whatever the assumed boundary conditions for the single-particle wavefunctions. This geometrical independence has been claimed to hold also for the electron–electron interaction as well as for other wavefunction-averaged quantities. Gold and Ghazaly (1990a) have shown, by comparing at a few q values the electron–electron interaction matrix elements with previous calculations made for a RQW (Kodama and Osaka 1986), the good agreement between the interaction potential in the lowest subband in both the geometries, using the scaling relation $l^2 = \pi R^2$ (l is the side of the square wire). We consider a rectangular wire with sides l_x and l_y in the infinite-barrier model.

Firstly, we have examined for this RQW the long-wavelength functional behaviour of the electron–electron interaction potential elements $V^{\square}_{\{m\}}(ql_x; c)$, where $\{m\} = \{m_1 m_2 m_3 m_4\}$ denotes the set of quantum numbers $m_i = 1, 2, \ldots$ of the four y-component planar wavefunctions (for the x component it is $n_i = 1$ hereafter) and $c \equiv l_y/l_x$. Reducing all these elements to cylindrical geometry by means of the relation $l_x = (\pi/c)^{1/2} R$ (R is the radius of the CQW), we have verified (both numerically and functionally) the following general results by choosing the values $R/a^* = 1, 3, 5, 10$ and $c = \frac{1}{2}, 1$

$$V^{\square}_{\{m,m',m',m\}}(ql_x; c) \approx \alpha(m, m'; c)\, V^{\bigcirc}_{\{m-1,m'-1,m-1,m-1\}}(qR),$$

$$V^{\square}_{\{m,m,m',m'\}}(ql_x; c) \approx V^{\bigcirc}_{\{m-1,m-1,m'-1,m'-1\}}(qR).$$

where the subscript $\square$ indicates the RQW and the superscript $\bigcirc$ indicates the CQW. The factors $\alpha(m, m'; c) \neq 1$, ranging from about 0.5 to about 1.3, are present only in the intersubband cases when $\Delta m \equiv |m - m'| \neq 0$. These α values are almost independent of q, so that they act on the curves as a quasirigid shift. We believe that the shift is related to the different subband energy separations in the respective geometries.

Another feature of interest is to make evident the possible remarkable differences in the excitation spectra between the two geometries. The above discussion convinced us that these geometrical peculiarities are not attributable to the effective electron–electron interaction. Geometrical features may therefore be manifested either because of different symmetry selection rules (decoupling of equation (2)) or from an intrinsic physical property of the plasmon excitations. The symmetry selection rules for the rectangular wire are $\sum (n_i + m_i) = \text{odd} \Rightarrow V^{\square}_{\{m\}} \equiv 0$. We follow those rules and use the expressions for the Fermi level, namely

$$E_{\mathrm{F}}^{[1]}(l_x, n, c) = \left(\frac{\pi n}{2}\right)^2 + \frac{\pi^2}{l_x^2}\left(1 + \frac{1}{c^2}\right), \tag{19}$$

$$E_{\mathrm{F}}^{[2]}(l_x, n, c) = \frac{\pi^2}{l_x^2}\left(1 + \frac{1}{c^2}\right) + \left(\frac{\pi n}{4}\right)^2 \left[1 + \left(\frac{\bar{n}_0(l_x, c)}{n}\right)^2\right]^2, \tag{20}$$

where equation (19) holds only if the first subband is populated, that is when $n \leqslant \bar{n}_0(l_x, c)$, and equation (20) holds only if the first and second subbands are occupied, that is when $\bar{n}_0(l_x, c) \leqslant n \leqslant \bar{n}_1(l_x, c)$. Here $\bar{n}_0(l_x, c) = 2 \times 3^{1/2}/l_x c$ and $\bar{n}_1(l_x, c) = 2(5^{1/2} + 8^{1/2})/l_x c$, with energies and lengths expressed in Ryd* and a^* respectively. In that framework, we have then calculated the plasmon excitations in both the 01 and the 012^0 models.

For the RQW in the 01 model, it can be proved that there are two intrasubband modes. They behave for $ql_x \ll 1$ as $\omega_-^{\square}(q) \approx (\hbar/m)(k_1 k_2)^{1/2} q$ (lower-energy plasmon) and $\omega_+(q) \approx \bar{\omega}_{\mathrm{S}}[-\ln(ql_x)]^{1/2} ql_x$ (upper-energy plasmon) respectively, where $\bar{\omega}_{\mathrm{S}}^2 = 2ne^2/m\varepsilon_{\mathrm{L}} l_x^2$ and $n = (2/\pi)(k_1 + k_2)$ is the linear particle density. Their dispersion equation is formally identical with equation (6). In particular, for the upper mode we obtain the same functional law as in the cylindrical wire (see equation (18 *a*)) while the lower mode, with linear dispersion, shows a difference with the cylindrical counterpart (see equation (4)). Indeed, we have performed a comparative calculation for $qa^* = 0.01$, setting $l_x = (\pi/c)^{1/2}R$ with $c = \frac{1}{2}$, and assuming equal densities in the two wires, $n = 1/a^*$. In figure 4, we plot the ratios $u(b) = \omega_+^\square(b)/\omega_+^\bigcirc(b)$ and $l(b) = \omega_-^\square(b)/\omega_-^\bigcirc(b)$ for the four intrasubband modes (+ for the upper branch and − for the lower branch), with the cylindrical radius $b \equiv R/a^*$, as far as the value at which the occupancy of the third subband starts. The different functional dependence on b is evident for the lower modes.

To explain this behaviour, one must consider how the mode coupling gives rise, in each wire, to the mixed excitations $\omega_\pm^{\square,\bigcirc}$. For small q, we found that the two modes, whose coupling causes the mixed frequencies, cross at some b value in the CQW, whereas in the RQW they are always well spaced. This means that the mode coupling is more efficient in the CQW than in the RQW. In particular, a lengthy calculation shows that $\omega_-^\bigcirc(b)$, after a maximum, decreases. On the contrary, $\omega_-^\square(b)$ monotonically increases. Alternatively, at $q \to 0$ we observe that the above behaviour is determined, through equations (19) and (20) and similar equations for the CQW, by the factor $(2k_{F0} + k_{F1})/(k_{F0} + 2k_{F1})$ in equation (4), which is absent in the RQW. From figure 4, it can be seen than $u(b)$ is ≈ 1 up to the point at which filling of the second subband in the CQW starts; then it increases until the same filling starts in the RQW; finally it shows an almost constant behaviour. In contrast, $l(b)$ shows a monotonic increase, well beyond the point at which occupancy of the second subband starts in the RQW.

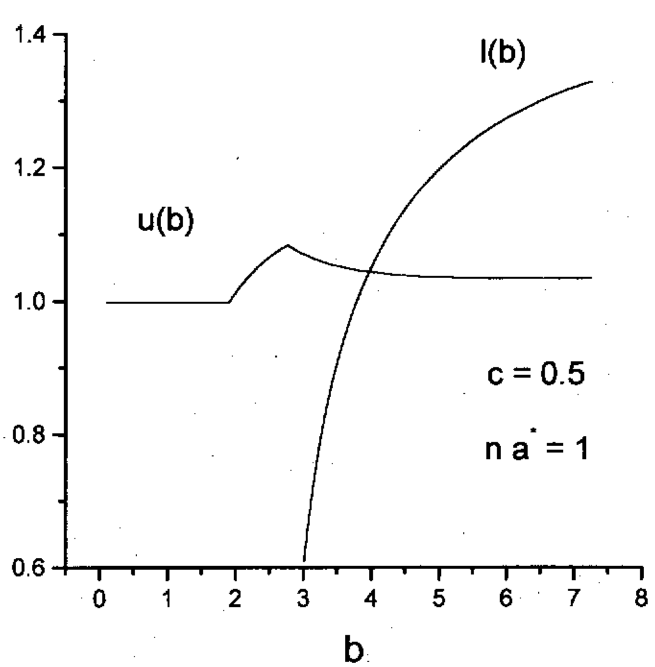

Figure 4. Plots of the ratios $u = \omega_+^\square/\omega_+^\bigcirc$ and $l = \omega_-^\square/\omega_-^\bigcirc$ of the intrasubband plasmon modes at $qa^* = 0.01$ versus $b = R/a^*$ in the 01 model in a CQW and a RQW. We set $l_x = (\pi/c)^{1/2}R$, $c = l_y/l_x = \frac{1}{2}$ and with equal densities $n = 1/a^*$ in both wires.

Therefore, lower-energy plasmons, with linear dispersion, are sensitive to the structure shape. The higher-energy plasmons $\omega_+^{\square,\bigcirc}$ at $q \rightarrow 0$ are just proportional to $n^{1/2}$ and are insensitive to the geometry. The $l(b)$ monotonic increase shown in figure 4 is then related to the different strengths in the mode coupling between intrasubband plasma excitations rather than to the respective selection rules, which, as mentioned above, lead to formally identical dispersion equations, at least for the case of two-subband systems.

A similar analysis has been extended to the 012^0 model. We have proved that, even with the inclusion of a third empty subband, no modification is found with respect to the previous results.

§ 6. Summary and conclusions

In this paper, we have studied the RPA collective plasmon spectrum of a Q1DEG confined in a quantum wire with cylindrical and rectangular confining potential shapes. The dispersion relations have been analyzed mainly in the long-wavelength limit, which allows the presence of undamped plasmons. Firstly, we have resolved the spectrum up to three occupied subbands in a CQW. When one takes into account the Coulomb interaction between states with opposite angular quantum numbers, we found, even in the two-occupied subband model, a new plasmon mode with a strictly linear dispersion law. The effect of the inclusion in the model of an empty third subband is relevant only in an enhancement of the depolarization shift of the first-to-second subband resonance. We have also shown that, in systems with three or more occupied subbands, the angular plasmons $\Delta l = 0$ obey two distinct dispersion laws: the upper branch is proportional to $[-\ln(qR)]^{1/2} qR$, and the lower branches are proportional to q.

We have examined the occurrence of a possible geometrical shaping effect, both on the effective Coulomb interactions and on the plasmon frequencies, by comparing these quantities in a CQW and in a RQW with the same cross-section areas. We have proved that, for the intrasubband interaction elements, the shape independence is very well verified, whereas the intersubband interaction elements are quasirigidity shifted owing to the respective energy subband separations in the two geometries. Thus, for various configurations, we have analyzed the plasmon modes, with particular regard given to the different intrasubband and/or intersubband excitation decoupling mechanism related to the respective symmetry selection rules. For the two wires, we have compared the plasmon spectrum in the 01 and 012^0 models. In the 01 model, we have shown the existence of a shaping confinement effect for the lower intrasubband plasmon related to a different strength in the model-coupling mechanism. In the 012^0 model, the inclusion of the empty third subband in that wire does not modify the behaviour of the intrasubband plasmons and so the shaping confinement effect still holds. We believe that the above shape effect can be observed in experimental investigations.

References

Agosti, D., Pederiva, F., Lipparini, E., and Takayanagi, K., 1998, *Phys. Rev.* B, **57**, 14 869.

Ando, T., Fowler, A. B., and Stern, F., 1982, *Rev. mod. Phys.*, **54**, 437.

Borges, A. N., Leao, S. A., and Hipolito, O., 1997, *Phys. Rev.* B, **55**, 4680.

Das Sarma, S., and Lai, W. Y., 1985, *Phys. Rev.* B, **32**, 1401.

Das Sarma, S., and Hwang, E. H., 1999, *Phys. Rev.* B, **59**, 10 730.

Ehrenreich, H., and Cohen, M., 1959, *Phys. Rev.*, **115**, 786.

GOLD, A., and GHAZALY, A., 1990a, *Phys. Rev.* B, **41**, 7626; 1990b, *ibid.*, **41**, 8318.
HAUPT, R., WENDLER, L., and PECHSTEDT, R., 1991, *Phys. Rev.* B, **44**, 13 635.
HU, G. Y., and O'CONNEL, R. F., 1990, *Phys. Rev.* B, **42**, 1290.
HWANG, E. H., and DAS SARMA, S., 1994, *Phys. Rev.* B, **50**, 17 267.
KODAMA, T., and OSAKA, Y. J., 1986, *J. Phys. Soc. Japan*, **55**, 3941.
KOTTHAUS, J. P., 1988, *Interfaces, Quantum Wells and Superlattices*, edited by C. R. Leavans and R. Taylor (New York: Plenum); 1989, *Nanostructure Physics and Fabrication*, edited by M. A. Reed and W. P. Kirk (Boston, Massachusetts: Academic Press).
LEE, J., and SPECTOR, H. N., 1985, *J. appl. Phys.*, **57**, 366.
LI, Q. P., and DAS SARMA, S., 1991, *Phys. Rev.* B, **43**, 11 768.
LI, Q. P., DAS SARMA, S., and JOYNT, R., 1992, *Phys. Rev.* B, **45**, 13 713.
MUTLUAY, N., and TANATAR, B., 1997, *Phys. Rev.* B, **55**, 6697.
PROETTO, C. R., 1992, *Phys. Rev.* B, **45**, 11 911.
REBOREDO, F. A., and PROETTO, C. R., 1994, *Phys. Rev.* B, **50**, 15 174; 1997, *ibid.*, **55**, 1680.
STERN, F., 1993, *The Physics of Low-Dimensional Semiconductor Structures*, edited by P. N. Butcher, N. H. March and M. P. Tosi (New York: Plenum), p. 177.
WENDLER, L., and GRIGORYAN, V. G., 1994, *Phys. Stat. sol.* (b), **181**, 133.
WENDLER, L., and HAUPT, R., 1995, *Phys. Rev.* B, **52**, 9031.
WENDLER, L., HAUPT, R., and PECHSTEDT, R., 1991, *Phys. Rev.* B, **43**, 14 669.
YU, H., and HERMANSON, J. C., 1990, *Phys. Rev.* B, **42**, 1496.